Long-Term Upper-Limb Prosthesis Myocontrol via High-Density sEMG and Incremental Learning

229 (2023) 212109

Contents lists available at ScienceDirect

Geoenergy Science and Engineering

journal homepage: www.sciencedirect.com/journal/geoenergy-science-and-engineering

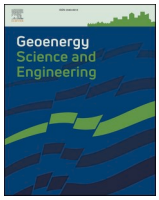

Deformation behavior of a regional shale formation from integrated laboratory and well data analysis: insights for underground fluid storage in northern Italy

Christoforos Benetatos [a,*], Vera Rocca [a], Francesca Verga [a], Luca Adinolfi [b], Francesco Marzano [b]

[a] Department of Environment, Land and Infrastructure Engineering, Faculty of Engineering, Politecnico di Torino, Corso Duca degli Abruzzi 24, 10129, Torino, Italy
[b] Stogit Division, Snam S.p.A., Piazza Santa Barbara 7, 20097, San Donato Milanese, Italy

ARTICLE INFO

Keywords:
Underground energy storage
Triaxial lab tests
Ultrasonic lab tests
Sonic logs
Deformation-depth relation
Diagenesis

ABSTRACT

The Po Plain in northern Italy is one of the most populated and industrialized European regions and hosts numerous gas fields, which have been in production for decades. Several reservoirs were subsequently converted into underground storage sites for natural gas (UGS) while others are currently candidates for future storage of CO_2 or H_2. In all cases, the reservoir caprock confining the fluids underground is the Argille del Santerno formation. The Argille del Santerno is a good-quality shale; it has a thickness ranging from several tens to hundreds of meters and it extends across a large part of the subsurface of the Po Plain. The part of the formation that acts as a caprock for the main reservoirs lies at an average depth of 1200–1500 m.

The scope of the present work was to obtain a sound evaluation of Young's modulus of the Argille del Santerno based on experimental data so as to describe the deformation behavior of the formation at current or prospective storage sites. To this end, we collected and analyzed a wide range of data from triaxial tests, ultrasonic laboratory analysis, and well logs from 6 different locations (corresponding to 6 reservoirs) in the Po Plain. Our dataset was enriched by publicly available log data, which we used for stratigraphic correlation purposes and identification of the Argille del Santerno throughout the Po Plain. An empirical relation between Young's modulus from log data and depth was inferred. Discrepancies among the results of the analyses are presented and discussed. We investigated the effects of alteration of cementation, diagenetic and aging behavior due to sampling operations, and the impact of the investigation techniques at the specimen scale (triaxial test and sonic wave propagation data) on Young's modulus values. This was done to explain the differences between lab and well values.

This paper provides a unique characterization of the Young's modulus of the Argille del Santerno at a regional scale, to serve as a reference for reliably predicting ground-level movements induced by underground storage activities.

1. Introduction

In the last decades, the Po Plain (northern Italy) has been subject to numerous studies that investigated every aspect of its complex geological evolution in detail from the tectonic and stratigraphic points of view (e.g., Fantoni and Franciosi, 2010; Ghielmi et al., 2010, 2103; Turrini et al., 2014; Amadori et al., 2018, 2019 and references therein) (Fig. 1). The particular tectonostratigraphic framework of the Po Plain has given birth to numerous hydrocarbon traps that have made Italy one of the countries that are richest in hydrocarbon fields in southern Europe. Most of the onshore gas reservoirs are located within the foredeep basins associated with the Apennine chain and along the Adriatic foreland (e.g., Casero, 2004; Picotti et al., 2007; Bertello et al., 2010; Cazzini et al., 2015). The hydrocarbon traps are usually a combination of anticline structures and faulting but stratigraphic traps are also common. In almost all the caprock-reservoir systems the sealing rock which prevents hydrocarbon migration towards overlying porous layers is the Argille del Santerno formation. During the Late Miocene/Early Pliocene periods, the deposition of basinal turbiditic-semipelagic clays or condensed clays occurred throughout the entire foreland area (Ghielmi et al., 2013). Such clays constitute the Argille del Santerno formation. The thickness of this formation varies between several tens to a few hundred meters in some depocenters across the Po Plain, reaching almost 1000 m near Bologna.

* Corresponding author.
E-mail address: christoforos.benetatos@polito.it (C. Benetatos).

https://doi.org/10.1016/j.geoen.2023.212109
Received 15 March 2023; Received in revised form 2 July 2023; Accepted 4 July 2023
Available online 8 July 2023

Nowadays, many of the gas fields have been converted into underground storage sites (UGS) while some depleted reservoirs have become candidates for future storage of CO_2 and H_2. In other cases, underground formations such as deep saline aquifers are under investigation with the same scope. In all cases, the presence of a sealing caprock is of fundamental importance to guarantee the confinement of the injected fluids. The ability of the Argille del Santerno to hydraulically confine hydrocarbons is confirmed by natural gas being trapped underground over geological eras. The study of the caprock physical and mechanical characteristics is of fundamental importance for assessing safety conditions when the caprock is subject to unloading and/or loading as a consequence of storage operations in the underlying reservoir. This induces pressure increase (fluid injection) and decrease (fluid withdrawal) even if the fluid is H_2 or CO_2 instead of natural gas.

Similar to famous international case studies, such as the Opalinus Clay in Switzerland (Soler, 2001;Bossart et al., 2004; Favero et al., 2016; Corkum and Martin, 2007; among the others or other cases worldwide (Gautam and Wong, 2006; Islam and Skalle, 2013; Gong et al., 2020)), the Argille del Santerno Formation has been the object of numerous, widespread yet local investigation surveys, often related to the hydrocarbon production target. As a consequence, unlike the Swiss case study, an overview of its physical properties at a larger scale is still missing.

A thorough characterization of the Argille del Santerno caprock has been undertaken within extensive research on safe H_2 and CO_2 storage (Benetatos et al., 2021). This paper focuses on one specific aspect of the characterization of the Argille del Santerno, namely the deformation behavior. Deformation data represent one of the key parameters for analyzing and forecasting the response of deep formations and the surface movements induced by storage operations.

The target of the study was to delineate a general deformation behavior of the Argille del Santerno at a regional scale through the analysis of all the available deformation data (mainly Young's modulus and Poisson's ratio). To this end, we collected more than 150 existing values of Young's modulus obtained via triaxial and ultrasonic lab tests: these values were determined from more than 60 specimens retrieved from the caprock of 6 hydrocarbon fields distributed across the Po Plain area (F1–F6 in Fig. 1), thus offering a wide sampling distribution. Furthermore, numerous log acquisitions were available in the same wells, allowing us to calculate the dynamic Young's modulus at the wellbore scale. All the values of Young's modulus were then compared. The effects of the sampling operations in terms of alteration of cementation, diagenetic and aging behavior, investigation techniques (triaxial test and sonic wave propagation), and acquisition scale were discussed to explain some discrepancies that were consistently found in Young's moduli. This dataset was further integrated and extended using public well log data from the VIDEPI database. The logs were used to reconstruct the regional stratigraphy and to identify the Argille del Santerno at the wellbore scale. Then, an empirical correlation of Young's modulus with depth was obtained and compared with previous findings. Finally, two representative case studies, for which static and dynamic Young's moduli were available, are presented and discussed to validate our findings. Based on the surveys in the areas of the Po Plain where UGS were developed, an insight on faulting is provided to highlight its spatial relationship to the Argille del Santerno deposits.

Representative static and dynamic models to forecast the reservoir performance (e.g., Rocca et al., 2019; Benetatos and Giglio, 2021) and to accurate predict ground-level movements are required by regulatory authorities as it can help to gain social acceptance for underground activities, especially in a highly urbanized and industrialized region such as the Po Plain. The present research can therefore define reliable input parameters for the geomechanical models used to calculate the deformation of underground systems and ground-level movements, caused by fluid injection and withdrawal.

2. Geological setting

Northern Italy is characterized by the presence of two large fold-and-thrust belts, the south-verging Southern Alps belt and the north-verging Northern Apennines belt (e.g., Pieri and Groppi, 1981; Castellarin et al., 1985; Carminati and Doglioni, 2012; Fantoni and Franciosi, 2009, 2010; Amadori et al., 2018, 2019). The Po Plain is situated on the Adria microplate which lies between the African and Eurasian plates and is considered the African plate promontory (Dercourt et al., 1986). The evolution of both belts was linked to the interaction between the African and Eurasian plates and resulted in the formation of the Neogene Po Plain foreland basin which is characterized by a complex tectonic and stratigraphic history.

During the Mesozoic era (Triassic-Jurassic period) the broader region experienced an extension phase (Bertotti et al., 1993; Fantoni and Franciosi, 2010) due to the opening of the Tethyan Ocean. This led to the creation of a series of platform basin systems where extensive deposition of carbonate successions occurred. This extension phase persisted until

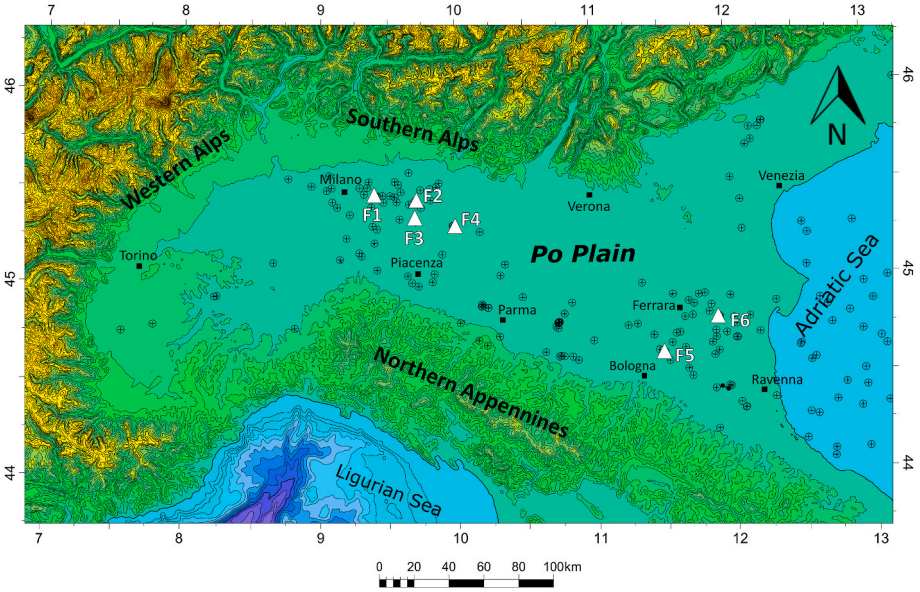

Fig. 1. Map of the Po Plain (Northern Italy). White triangles indicate the sampled locations while the crossed circles indicate the location of regional wells with publicly available sonic log data (UNMIG).

the Early Paleogene when compressional tectonics affected the area due to the convergence between the European plate and Adria microplate. During the Cenozoic, the subsurface architecture of the Po Plain and the northern Adriatic Sea was shaped by the evolution of fold-and-thrust belts, thrust-top basins, and foreland areas. Compressional tectonics affected the area since the Middle Eocene characterized by the development of thrust faults in the Southern Alps front while during the Oligocene-Late Miocene by the development of thrust fault systems at the Northern Apennines front (e.g., Carminati et al., 2012; Maesano and D'Ambrogi, 2016). The two main fronts eventually became nearly parallel, facing each other, and locally collided during the Messinian period (e.g., Carminati and Doglioni, 2012; Toscani et al., 2014 and references therein). Since then, only the Northern Apennine front remained tectonically active.

From the stratigraphic point of view, the deposition of carbonatic sequences during the Mesozoic period was followed by thick Cenozoic successions of clastic sediments, made up of sands and shales that were deposited during the thrust belt activity. In the eastern part of the basin (northern Adriatic) thick marl-dominated sequences developed within shelfal, marginal, and marine successions while in the central part of the Po Plain (Apennine foredeep) thick sequences dominated by sand were deposited as turbidites.

During the Early Pliocene, an significant tectonic episode impacted the entire Apennine fold-and-thrust-belt resulting in rapid subsidence of the foreland areas and a sudden marine transgression. This transgression led to the deposition of marine clays in a large portion of the foreland, known as Argille del Santerno. During this time, the Apennine foredeep was divided into separate depocenters that forming a large, elongated basin, referred to as Modern Apennine Foredeep (MAF) (Ghielmi et al., 2010, 2013), stretching parallel to the main axis of the Apennines Mountain range. The basin underwent little or no deformation from the Late Miocene to today. Since the Early Pliocene, thick sand-dominated turbiditic sequences deposited in the migrating foredeep while shale deposition occurred in the foreland, foreland ramps, and paleo-high areas. During the Late Pliocene–Pleistocene period, the buried fold-and-thrust-belt experienced a complete deformation and at the same time, a new foredeep basin was created in the northern Adriatic Sea (Ghielmi et al., 2010).

During the Middle-Late Pleistocene, the growth of the buried belt was decreased and there was a rapid southeastward progradation of slope, shelfal and coastal deposits. This transitioned the sedimentation in the Po Plain from marine to continental resulting in the basin being complete filled, and the migration of the foredeep depocenters towards the central Adriatic Sea (e.g. Bertello et al., 2010; Fantoni and Franciosi, 2010; Ghielmi et al., 2010). In general, during the period from Late Messinian to Pleistocene, foredeep turbidites of the Po Plain-Adriatic foredeep reach a maximum thickness of 7000–8000 m (Cazzini et al., 2015).

The main stratigraphic units in the Po Plain, starting from the oldest to the youngest are:

- The Variscan crystalline basement, is overlaid by the carbonate platform (mostly limestone and dolomites) of the Triassic to Eocene age. During the Miocene, it was deposited the Marne di Gallare Fm., which consists mostly of marls and clayey/sandy marls with sand intercalations. From Late Miocene to the Late Pliocene, the basin experienced clastic formations deposition that include the Santerno Fm. (clay-rich units), sand-rich formations or sand/shale alternates (e.g. Bagnolo Fm., Porto Garibaldi Fm., Porto Corsini Fm.). In more recent times during the Pleistocene sand-rich sequences were deposited consisting of sands with clay interlayers (Sabbie di Asti) while the younger part of the stratigraphic record is occupied by recent clastic deposits of gravel and sands with clay intercalations of the continental, deltaic, and marine environment (Ghielmi et al., 2010 and references therein).

In Fig. 2 the upper portion of the stratigraphic record until the base of the Pliocene is presented. This geologic time frame hosts the majority of the hydrocarbon reservoirs in Po Plain.

The geologic formation under investigation in the present study is the Argille del Santerno (Santerno/Argille Azzurre Fm. in Fig. 2), which consists of clay-rich units mostly made of silty clays with a small percentage of sand.

3. Dataset

The dataset comprises well logs and laboratory data from wells drilled in various areas of the Po Plain basin (Fig. 1). The well data includes both propriety and public well logs. Public data were retrieved from the VIDEPI database (ViDEPI, 2023) and were utilized for the reconstruction the regional stratigraphy and the identification of the Argille del Santerno Fm. The calculation of dynamic elastic moduli from well logs was based on the analysis of sonic P-wave logs from Benetatos et al. (2019). Triaxial and ultrasonic lab tests were performed on numerous specimens extracted from the Argille del Santerno.

The VIDEPI database is a project managed by the Italian Geological Society (SGI) and the Ministry of Economic Development of Italy, funded by the Italian Petroleum and Mining Industry Association (Assomineraria). It includes a significant number of documents related to hydrocarbon exploration in the Italian peninsula including technical reports, over 2200 well log profiles (1:1000), and around 3000 seismic sections from the onshore and offshore areas of Italy. Well profile data were all downloaded and digitized. The spontaneous potential (SP) and gamma-ray (GR) logs were used for stratigraphic correlation purposes and lithological identification. Resistivity logs (Res) were used to identify possible hydrocarbon-bearing intervals and exclude them from the analysis since the presence of hydrocarbon alters the measured rock properties. Sonic logs (Sonic) were used for the sonic velocity analysis and the calculation of the dynamic elastic moduli. To ensure consistency and the best possible correlation between laboratory and well data, only proprietary log data were used in the subsequent analysis.

The cores used for laboratory analyses were retrieved from depths ranging between 1000 m and 1700 m. Static values were derived from deformation measurements obtained performing triaxial compressive tests, with increasing confining pressures from 5 MPa to 25 MPa (increments of 5 or 10 MPa). The standard test conditions involved a single loading phase, with only a limited number of experiments conducted under cyclical unloading-reloading confinement. Given the clayey characteristics of the caprock, undrained conditions were maintained during testing. Sonic measurements were taken during the compressive tests at confining pressures between 5 MPa and 20 MPa enabling the calculation of the dynamic Young's modulus at the plug scale. For the dataset construction, lab data were selected based on the representativeness of the cores and test confinement conditions; only the values obtained from the first loading cycle of the triaxial tests were considered to maintain coherence. The dataset consists of 82 static values of Young's modulus acquired from 41 laboratory tests on samples extracted from 11 wells (6 reservoirs), and nearly 64 dynamic values of Young's modulus acquired from 18 ultrasonic tests on samples retrieved from 3 wells (1 reservoir).

4. Methodological approach

The pseudo-elastic parameters of clastic formations are linked to several factors such as: the nature and the structure of the porous media, the saturating fluids, and the *in-situ* stress conditions. These factors can be also influenced by external parameters such as the induced strain amplitude. In the scientific literature can be found an extensive research on the effects of lithology, saturating fluid, and *in-situ* stress conditions on deformation parameters (i.e. Jardine et al., 1984; Fjaer et al., 2008; Lancellotta, 2012). In the Italian territory, the Po Plain basin has been the subject of extended experimental and theoretical research by various

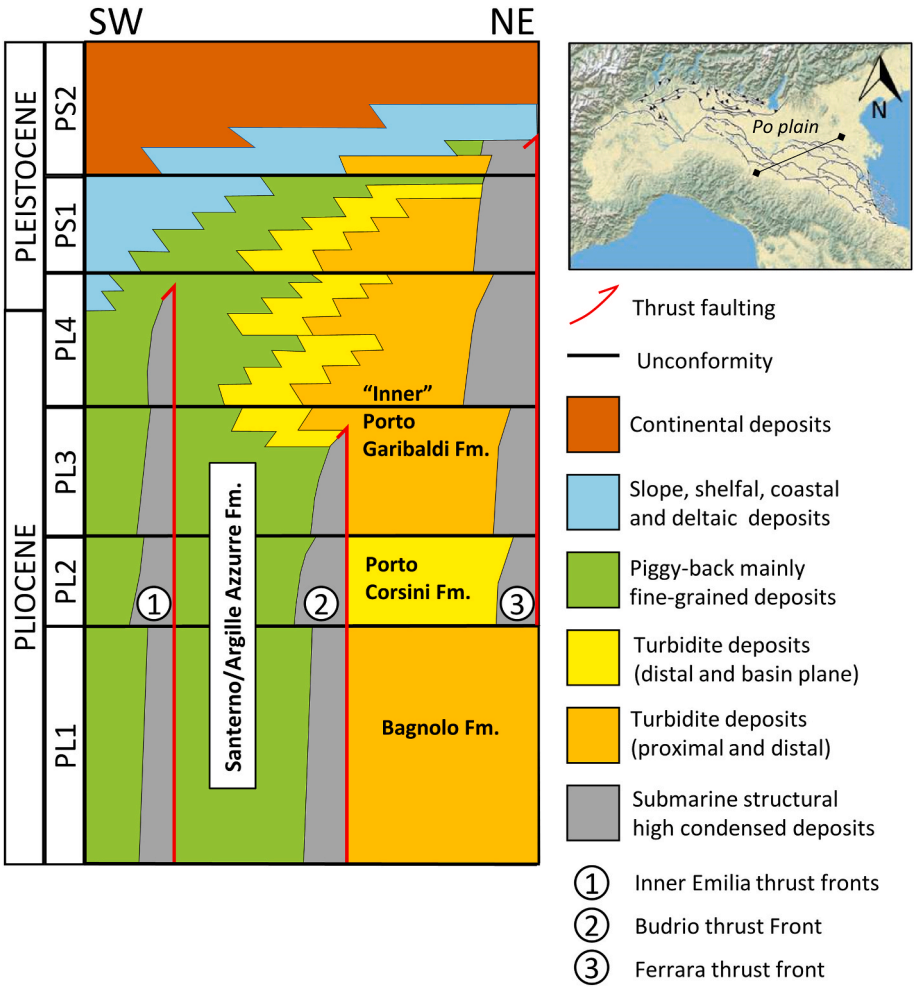

Fig. 2. Simplified Plio-Pleistocene stratigraphic framework for the central part of the Po Plain along a general SE-NE direction shown in the inset map (Fig. modified from Ghielmi et al., 2013). The names of the stratigraphic sequences are after Ghielmi et al. (2010, 2013).

scientific groups, such as, Baù et al. (2002), Ferronato et al. (2002); Teatini et al. (2011); Cardu et al. (2012); Codegone et al. (2016); Coti et al. (2018); Antoncecchi et al. (2021). For example, Baù et al. (2002) statistically analyzed *in-situ* deformation measurements carried out using the radioactive marker technique in different hydrocarbon wells drilled in the off-shore area of the Po plain basin. They established a correlation between the uniaxial compressibility, C_m, and the effective vertical stress, σ'_v as follows

$$C_m = 1.0044\ 10^{-2}\ \sigma'^{-1.1347}_{v} \quad [MPa^{-1}] \tag{1}$$

The compressibility derived from marker measurements was assumed to represent the first loading cycle. Uniaxial compressibility is related to the Young's modulus, E, and to the Poisson's ratio, ν, through the following equation:

$$C_m = \frac{1}{E}\frac{(1+\nu)(1-2\nu)}{1-\nu} \tag{2}$$

Baù et al. (2002) studied a depth interval ranging from 1000 m to 4000 m ssl, which primarily comprised silty to fine-grained sandstone formations. Their results indicated a negligible impact of lithology variation compared to depth variations on the elastic modulus values. The findings of Baù et al. (2002) were used as a basis for comparison in the present research.

The effects of investigation techniques (i.e., triaxial test and sonic wave propagation) were inferred through the analysis of laboratory data. The standard terminology distinguishes static moduli, E_S, as the values obtained from stress and strain measurements in rock mechanical tests in the laboratory, from the dynamic moduli, E_D, that is obtained from acoustic velocity data (Lancellotta, 2012). The latter better represent material deformation behavior at (very) small strains; while the former are associated with increasing strain levels. In medium to poorly consolidated rocks, the difference between static and dynamic values can be an order of magnitude or more (Fjaer et al., 2008; Marzano et al., 2020).

The evaluation of dynamic moduli can be performed at either the core or the well scale, and comparing the two sets of values can provide insights into scale effects. For the calculation of Young's modulus from the available sonic logs, the following procedure was followed. The original sonic log reports the formation slowness, in μsec/ft, which were converted to P-wave sonic velocities (km/sec). Since S-wave measurements were absent, the formula proposed by Castagna et al. (1993) was used to calculate the S-wave sonic velocities necessary for the calculation of the dynamic Young's modulus:

$$v_s = 0.804\ v_p - 0.865 \tag{3}$$

where v_p is the sonic P- wave velocity.

The dynamic Young's modulus, E_D, was calculated using the formula proposed by Darracott and Orr (1976), Fjaer et al. (2008) and Martínez-Martínez et al. (2012):

$$E_D = \rho v_s^2 \frac{3v_p^2 - 4v_s^2}{v_p^2 - v_s^2} \tag{4}$$

where ρ is the density of the rock and it was calculated following Gardner et al. (1974) who proposed the following formula for sedimentary rocks:

$$\rho = 1.74 v_p^{0.25} \quad (5)$$

The theory of seismic wave propagation was also adopted for the calculation of the dynamic elastic moduli at the core scale, and the sonic tests provided both the P-wave and S-wave measurements.

5. Results and discussion

The Young's modulus values are analyzed and discussed considering the distribution in relation to the induced strain magnitude (i.e, acquisition methodologies) and the investigated scale (namely, specimen or well). The effects of the measurement procedure were quantified based on the laboratory data. Furthermore, the influence of the confining stress applied during the determination of E_S and E_D in the laboratory was analyzed. The relationship between Young's modulus values and depth was also investigated, for both lab and log data, leading to the identification of an empirical correlation. Furthermore, two case studies are presented where static and dynamic values (when available), obtained through laboratory tests, are compared with dynamic data coming from well logs at the same wells. X-Ray Diffraction Analysis data were used to gain insight into diagenetic processes. Lastly, an overview of the characteristics of the main thrust faults of the Po Plain is presented.

5.1. Young modulus values distribution

The Young's moduli were measured on several samples (labeled from A to AD) under different levels of confining stresses. The core samples consistently indicated that the caprock is composed of rather homogeneous and unfractured shales. Fig. 3 (left) shows the distribution of the static Young's modulus: data are clustered around a mean value equal to 1.45 GPa with a standard deviation equal to ± 0.99 GPa. In the same figure (Fig. 3 right), the effects of the confining stress on Young's Modulus are illustrated. The confining stresses range from 5 to 25 MPa with incremental steps of 5 or 10 MPa. Although these effects are significant it is important to note that the Young's modulus values are extremely low, rendering the variations induced by confining stresses negligible for practical applications (such as subsidence analyses).

Fig. 4 shows the distribution of the static Poisson's ratio obtained from triaxial tests: during the quality check phase, numerous tests were excluded because they gave unreliable values (higher than 0.5). A mean value equal to 0.35 was derived by a statistical analysis of the data. This value was adopted for further investigation.

The dynamic values of Young's modulus were determined by performing ultrasonic lab tests on numerous plugs from 3 wells in the same reservoir, with increasing confining pressures in the range of [5–30] MPa. Fig. 5 presents the comparison between static and dynamic values for this particular subset of data. The distribution of the static Young's moduli shows a mean value equal to 1.77 GPa with a standard deviation equal to ±0.61 MPa, in agreement with the values derived from the

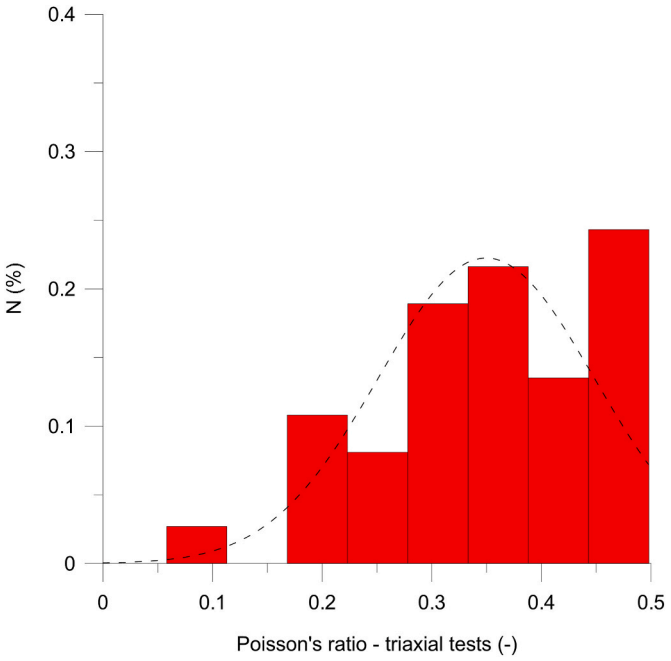

Fig. 4. Distribution of the static Poisson'ratio from lab tests. (N is the relative frequency).

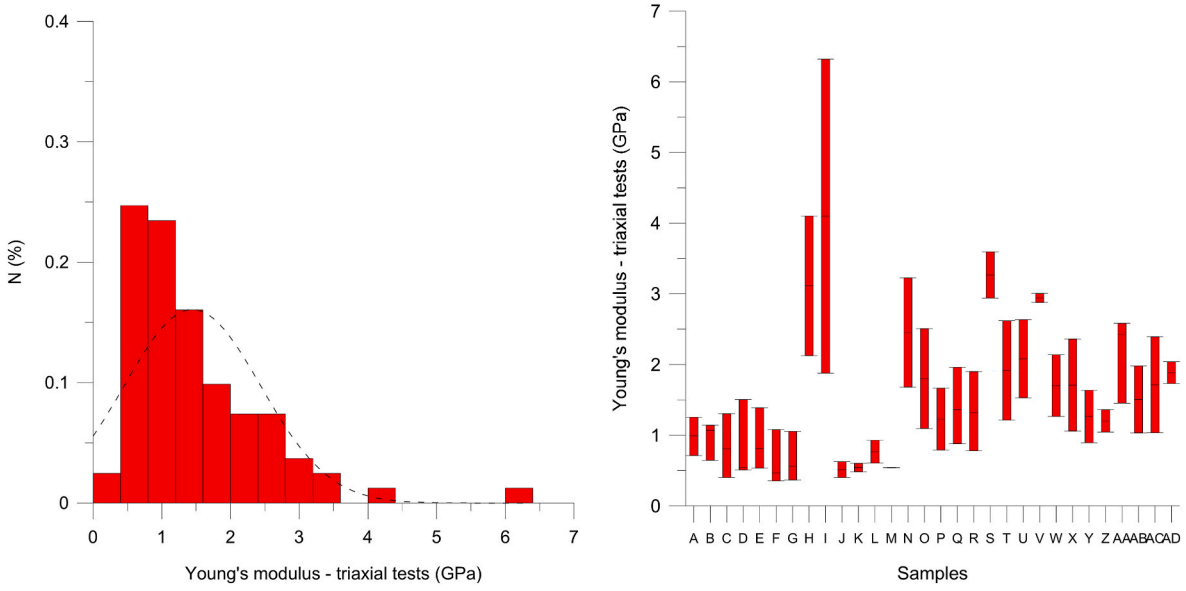

Fig. 3. (Left) Distribution of the static Young's Moduli from lab tests (N is the relative frequency). (Right) Effect of confining stress on Young's moduli with confinements in the range of [5–25] MPa (letters refer to samples).

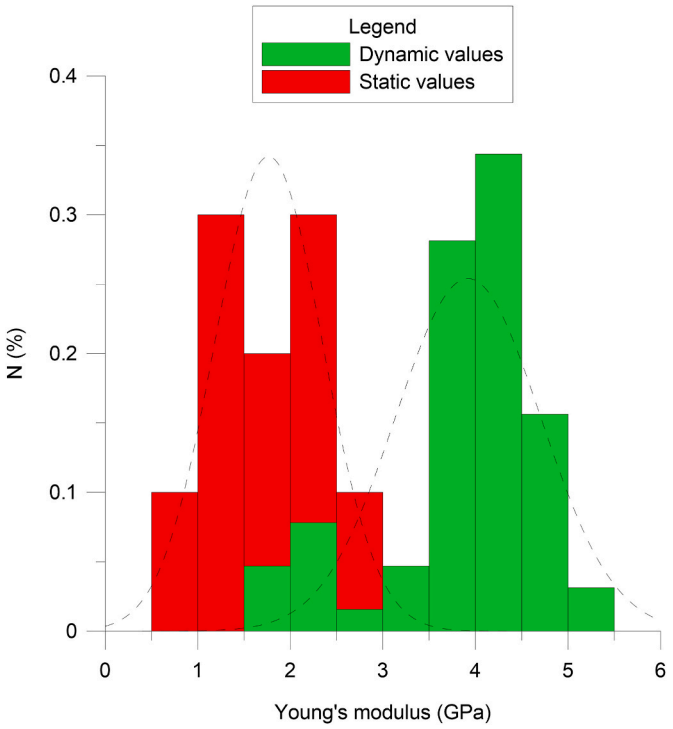

Fig. 5. Comparison between static and dynamic Young's Modulus values from lab tests. (N is the relative frequency).

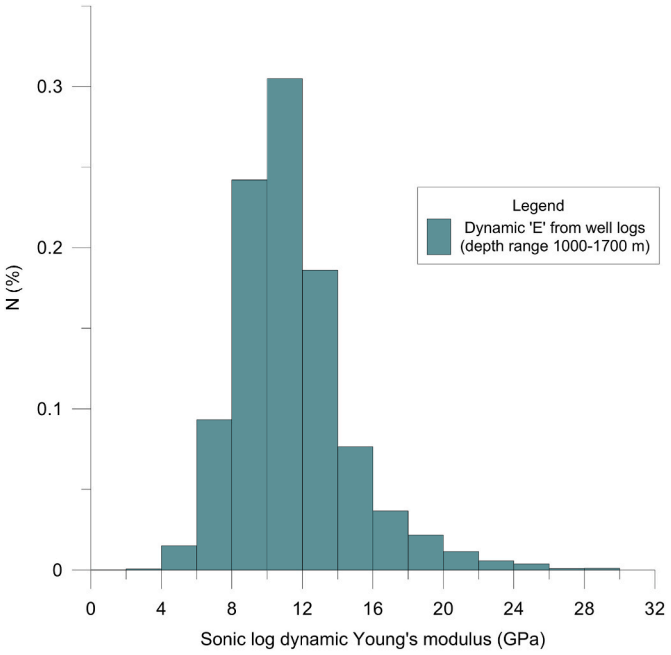

Fig. 7. Dynamic Young's Modulus distribution from sonic logs. (N is the relative frequency).

complete dataset (Fig. 3). The distribution of the dynamic values is characterized by a mean equal to 3.92 GPa with a standard deviation of ±0.79 GPa. Furthermore, in accordance with the theoretical literature (Fjaer et al., 2008), Fig. 6 depicts the effect of confinement stresses within the range of 10–20 MPa with incremental stress steps of 5 or 10 MPa. This effect is evident in the case of lower static values (samples from A to D). However, it becomes negligible in the case of higher dynamic moduli (samples from A* to D*).

Fig. 7 presents the distribution of the dynamic Young's modulus calculated from the sonic logs in the depth interval 1000–1700 m. The values are concentrated mostly between 8 and 14 GPa. It is worth noting that there is a significant difference compared to the values obtained from lab test analyses. This difference can eventually attributed, to scale effects, which will be further discussed in the following sections.

5.2. Depth-related Young's modulus variations

In Fig. 8 the comparison between depth-related static values and the experimental correlation derived by Baù et al. (2002) as expressed by eq. (2), is presented.

The correlation proposed by Baù et al. (2002) was applied assuming Poisson's ratio equal to 0.35 and 0.3, respectively. The first Poisson's ratio was derived statistically from our analysis of the lab data, while the second is a reference value for clastic consolidated material available in

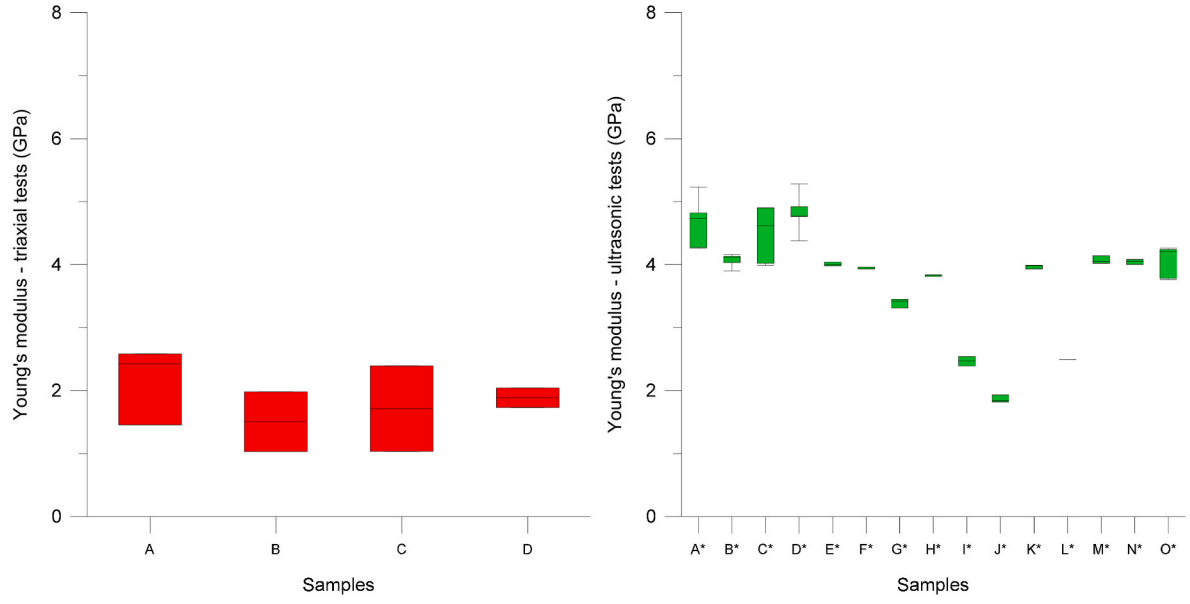

Fig. 6. Effect of confining stress on Young's modulus from lab tests in case of static (left) and dynamic values (right) (letters refer to samples and N is the relative frequency).

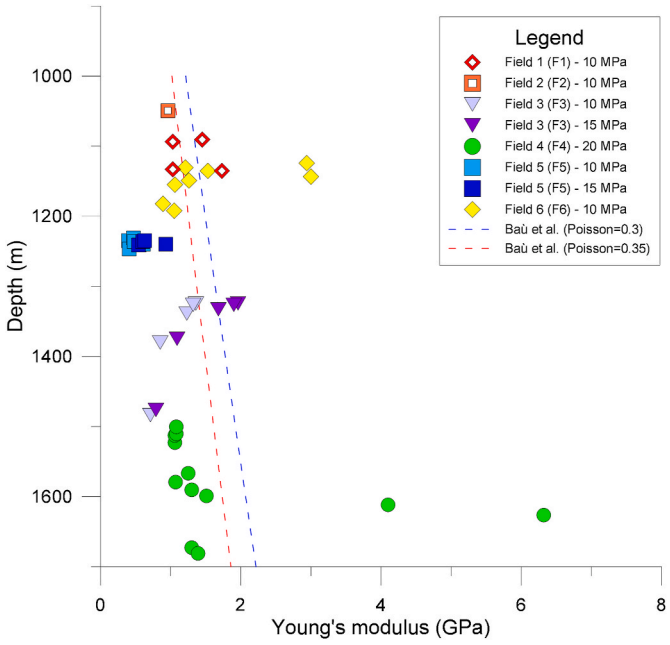

Fig. 8. Comparison between static Young's modulus values vs depth and Baù et al. (2002) relation. The confining pressure for the laboratory analyses is indicated next to each group of samples.

the technical literature (Fjaer et al., 2008). The variation of rock density with depth was determined using equation (5). Overall, the data show consistency with only minor discrepancies observed at higher investigated depths. However, it is important to note that the lab values appear to be unrelated with depth for the analyzed depth interval.

In Fig. 9 a comparison is made between the static lab data and the dynamic values from the sonic logs, clearly illustrating a difference of one order of magnitude. For this analysis we selected only the well log values that corresponded to the fields where static measurements were also available or nearby. As expected, the results demonstrate a continuous increase of the dynamic Young's modulus values with depth following the general trend of the sonic velocities.

The interval transit time (μs/ft) values from the sonic log show a continuous decrease with depth due to the compaction of the sedimentary layers, which also results into an increase in rock density. Benetatos et al. (2019) analyzed data coming from a large dataset of wells from the Po Plain (data available in Livani et al., 2023): it was shown the characteristic reduction of the transit time values, reaching approximately 40 μs/ft at around 7 km depth, which corresponds to the deepest logged part of the wellbore. Since sonic velocity is inversely proportional to interval transit time, we observe an increase in the velocities moving deeper in the subsurface geological formations. We converted all transit time values into sonic velocities (km/sec), keeping only the values that correspond to the shale intervals, and then used them to calculate the dynamic Young's modulus. The S-wave velocity and the density of the formations were determined through the empirical relations, presented in Section 3.

At a depth of approximately 1600 m, a change in the slope of Young's modulus vs depth relation is observed: it can be attributed to the gradual transition from shale to conglomerate lithologies observed in field 4 (F4 in Fig. 1). The sonic log values corresponding to shale lithologies are probably affected by the sonic velocities related to the conglomerate lithologies. The higher velocities that characterize the conglomerate lithologies contribute to the sudden increase of the sonic velocities and thus of the dynamic Young's modulus values.

To derive an empirical correlation between the dynamic Young's modulus and depth for the Po Plain, a linear regression analysis was performed within the depth interval of 1000–1600 m. The log data from the last 100 m was excluded from the linear regression analysis to eliminate the influence of the conglomerate lithologies in the 1600–1700 m interval. The identified correlation between the *in-situ* dynamic Young's modulus E_D and depth is:

$$E_{D(in\ situ)} = 0.0127\, d - 5 \quad (6)$$

where depth (d) is in (m) and E_D in (GPa).

The data and the correlation are shown in Fig. 10.

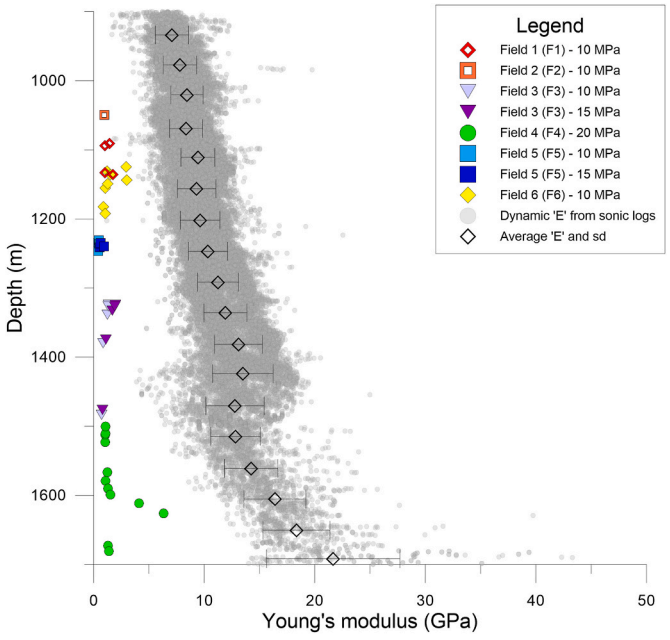

Fig. 9. Comparison between the Static Young's modulus from core samples and dynamic Young's modulus from sonic wells as a function of depth. The confining pressure for the laboratory analyses is indicated next to each group of samples.

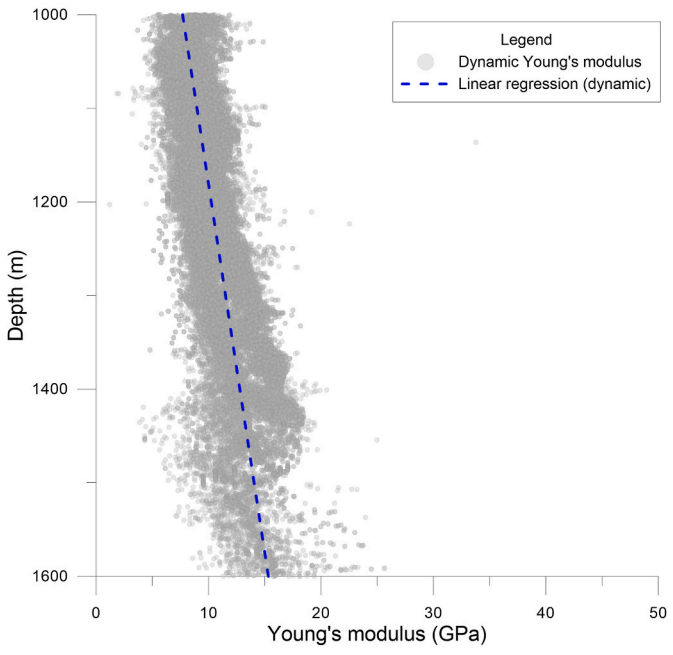

Fig. 10. Linear regression on the dynamic Young's modulus values calculated from sonic well logs as a function of depth, for the depth range 1000–1600 m.

5.3. Case studies

Two case studies are presented in Figs. 11 and 13, related to the fields F1 and F3 respectively, for which both lab and log Young's modulus values were available at the same wells.

In the case study related to field F1 (Fig. 11) the correlation between depth oand the Young's modulus values is not significant for the laboratory values due to the limited investigated depth interval (approx. 80 m). However, a slight correlation can be observed for the well log values. The average ratio E_D/E_S at the lab scale is approximately 3 and the same ratio is also observed between log and lab dynamic values. Therefore the Young's modulus values obtained from well logs are approximately one order of magnitude higher than those obtained from the triaxial tests in the laboratory. Additionally, in field F1 the availability of both static and dynamic laboratory measurements at the same well allowed the definition of a mathematical relationship between them (Fig. 12). To this end, we used only the samples for which static and dynamic measurements were available at the same depth and we also added the samples tested at a higher confinement pressure (20 MPa).

Similar observations were made also at Field F3, where no ultrasonic data at the plug scale were available. Due to the wider investigated depth interval, the effect of depth on log values is more evident (Fig. 13).

These case studies show the differences between the lab and well log values of Young's modulus, with the well log values generally being higher and showing a stronger correlation with depth. The ratio between dynamic and static Young's moduli provides insights into the scale effects and the differences in measurement techniques.

5.4. Diagenetic processes

To verify the occurrence of diagenetic processes, we followed the approach described by Favero et al. (2016), who examined the mineralogical composition of the rock samples. According to Ali et al. (2010), diagenetic processes can lead to (1) recrystallization of the particles without any composition alterations; (2) precipitation of new minerals due to the circulation of pore fluids, and (3) replacement, which occurs

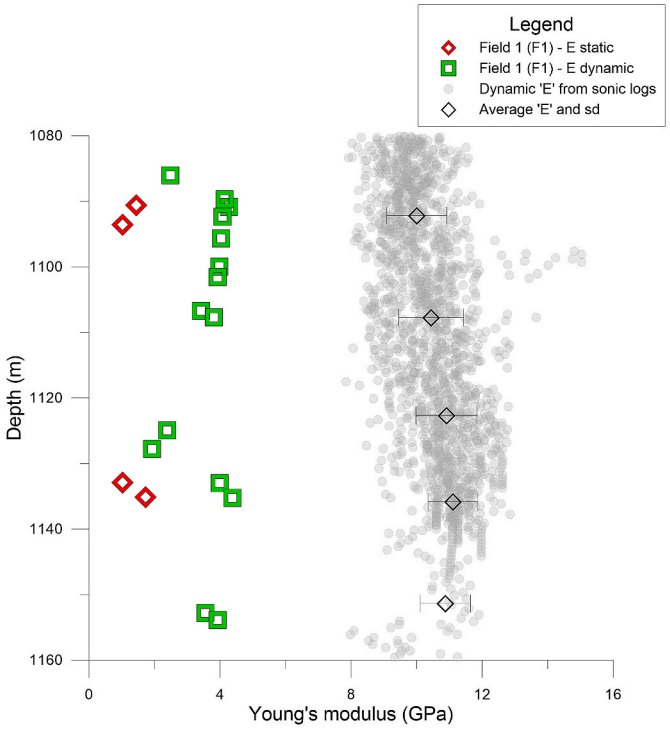

Fig. 11. Comparison between static and dynamic Young's moduli from samples and dynamic Young's moduli from sonic logs, at the same well, at field F1.

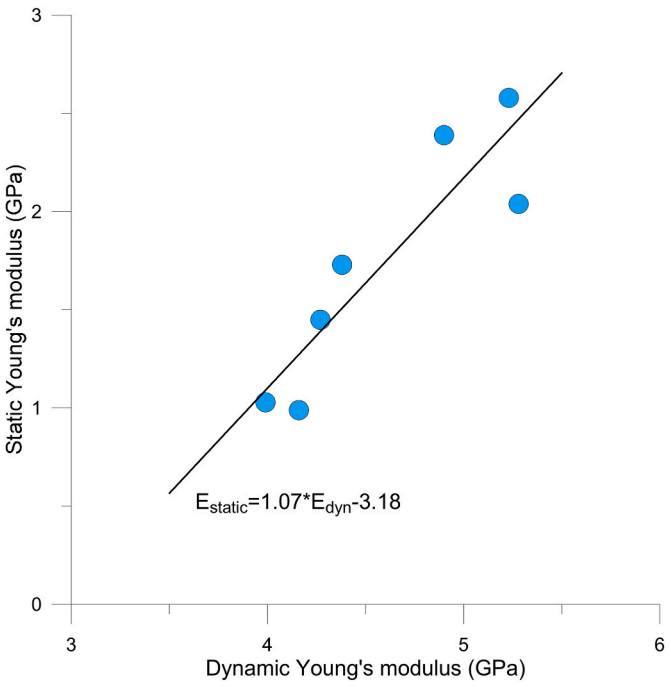

Fig. 12. Cross-plot of dynamic versus static measurements of Young's modulus at the same depth, at field F1.

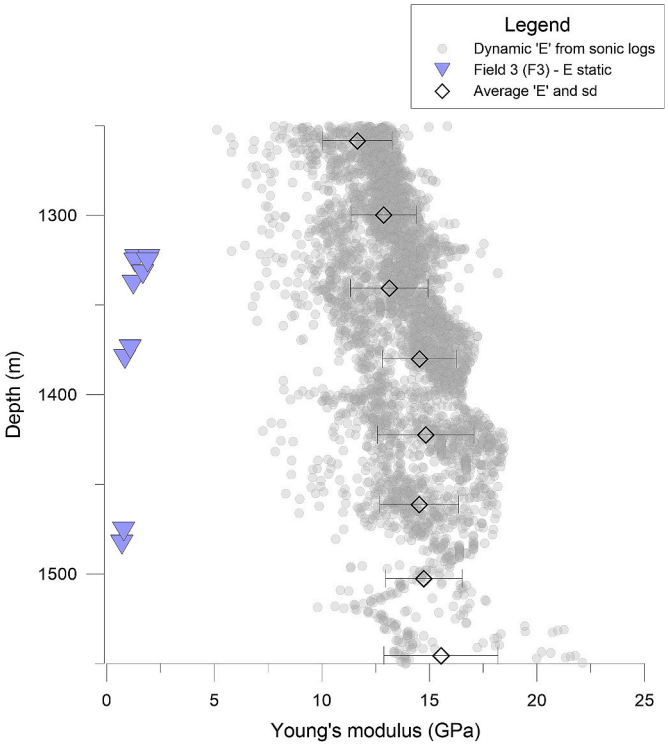

Fig. 13. Comparison between static Young's moduli from samples and dynamic Young's moduli from sonic logs, at the same well, at field F3.

if the sediment particles change their chemical composition. The first two processes usually affect carbonate and quartz grains, while the third one mostly affects calcite that is transformed into dolomite (dolomitization). The identification of diagenetic processes in shale samples can be deduced from the increase of the quartz and dolomite quantities in the tested samples. In total, we collected 37 measurements taken from

cores extracted from two wells. We observed a general increase with depth in quartz and dolomite concentrations in samples taken at depths spanning the range from 1000 m to almost 1700 m (Fig. 14). The trend suggests possible influence of diagenetic effects. However, it is worth noting that the deepest sample (core 6 in Fig. 14) exhibits unexpectedly low values of quartz and dolomite compared to the samples retrieved at shallower depths. To investigate further, we examined the high-resolution density log (RHO8) recorded at the same well (Fig. 15). The log indicates an upper part of core 6 characterized by low densities that can be attributed to a higher porosity. Possibly sandy lithologies prevail at those depths potentially impacting the mineralogical analysis of the samples.

5.5. Regional faulting

The Po Plain basin is characterized by the presence of the buried fronts of the southern Alps and of the northern Apennines which intersect in central Lombardy over an extensive E-W area of approximately 100 km length.

Many studies have been dedicated to the Southern Alpine margin of the Po Plain foreland (e.g., Quattrone et al., 1990; Fantoni et al., 2004; Bresciani and Perotti, 2014; Toscani et al., 2014). Amadori et al. (2018) performed a palaeo-topographic reconstruction of the Po Plain and the northern Adriatic Sea during the Messinian salinity crisis and they defined the Latest Messinian Unconformity (LMU) surface through the interpretation of seismic lines and well data. The structural system of the area demonstrates that in the area of the convergence between the two buried fronts, the southern Alpine structures remain active until the Late Messinian. Similar observations were reported by Bresciani and Perotti (2014) in the area of the Romanengo anticline showing that the buried thrusts reach the base of Messinian deposits but do not affect the overlying Argille del Santerno (Fig. 16).

The northern Apennines margin is a fold-and-thrust mountain range that was generated during the Eocene period due to the convergence of the African and European plates (Carminati and Doglioni, 2012). It consists of three main arcs, known as the Monferrato, the Emilian, and the Ferrara arcs, arranged from west to east. The activity of the northern Apennine fronts is currently concentrated along the thrust faults buried under the Po Plain and along the partially exposed structures that form the mountain front delimiting the Plain to the southwest (Maesano et al., 2015). In recent years, numerous structural studies have been carried out at a regional scale based on re-interpretations of seismic lines (e.g. Picotti and Pazzaglia, 2008). Boccaletti et al. (2011) focused on the external part of the Northern Apennines using an integrated analysis of

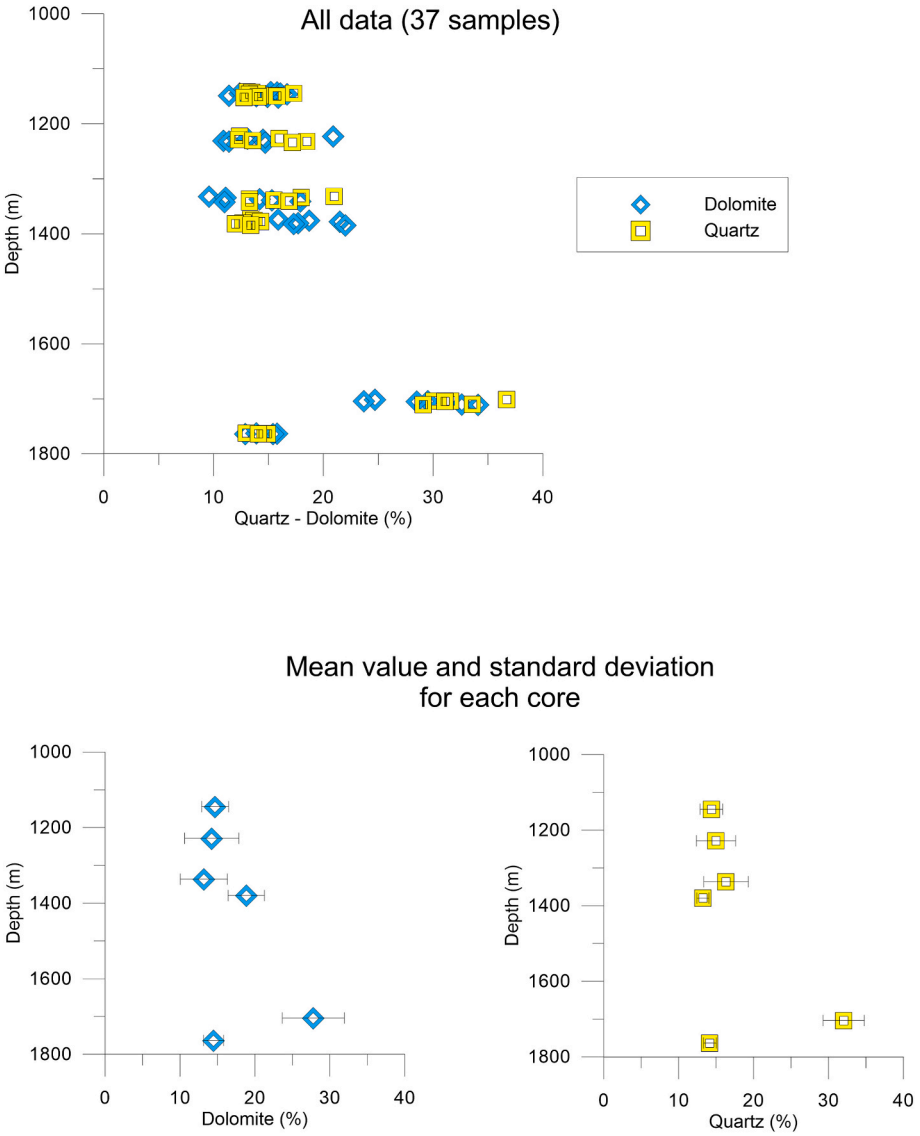

Fig. 14. Mineralogical composition of the tested shale samples versus depth: (top) all data, (bottom) mean values and standard deviations.

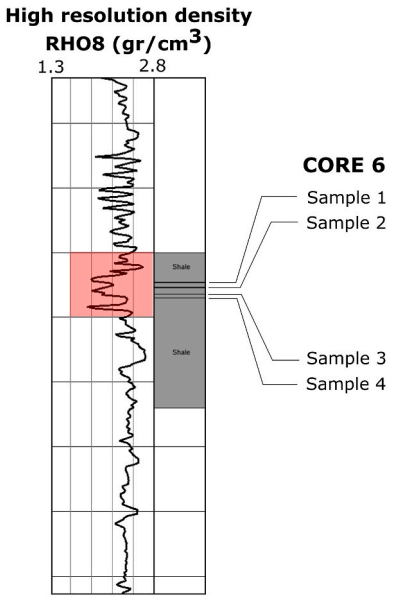

Fig. 15. Density log (RHO8) and location of core 6. It can be noted that the part of the core where the samples were taken shows unusually low density values indicating higher porosity or the presence of local fractures, likely induced by drilling.

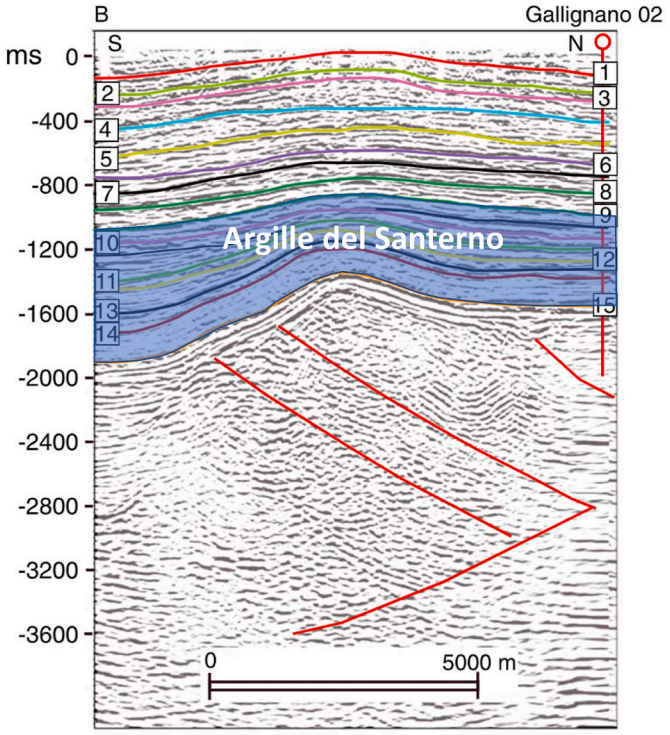

Fig. 16. Cross section of the Romanengo anticline where 15 stratigraphic markers from the well Gallignano 02 are also shown. The markers from 9 to 15 (blue color) indicate the Argille del Santerno stratigraphic zone (fig. modified from Bresciani and Perotti, 2014).

morphotectonic, geological-structural, and stratigraphic data compared to the current seismicity of the area. Their work includes a seismic section illustrating that the main thrusts in the region extend to the Early Pleistocene without reaching the Top of the Argille del Santerno Fm. And thus not causing displacement in the Quaternary sequence (Fig. 17).

The examples presented above, derived from seismic interpretation and structural analysis, indicate that in the proximity of the hydrocarbon fields (located in the broader studied areas) the vertical continuity of the Argille del Santerno Fm. is not compromised by the presence of major faults, which they terminate below the top of the shale deposits. Thus, the sealing capacity of the Argille del Santerno is guaranteed.

5.6. *Final remarks on Young's moduli*

The mechanical properties of the Argille del Santerno are the result of the sedimentation, burial and diagenesis processes that occurred in their geological history. Both the mechanical loading and diagenetic processes which developed during their burial/uplift/erosion history contribute to the mechanical behavior of the shale. As well documented in the technical literature (Gibson, 1958; Skempton, 1969; Jones and Addis, 1985; Burland, J., 1990, among others), the mechanical load and consequent rock compaction affect the formation porosity and stiffness, together with the rock fluid-flow and mechanical resistance. Superimposed diagenetic processes are also responsible for the cementation and bounding of the material structure, which ultimately impact the petrophysical properties and deformation behavior of the formations.

Core sampling and remolding processes can modify the structure of the original material, and consequently influence the experimental results (Schmertmann, 1991; Hong et al., 2012; Favero et al., 2016, among others): if the cementation and the diagenetic bounds are compromised by these processes, lab experiments show higher porosity and compressibility compared to the undisturbed formation. Furthermore, swelling and creep phenomena are mitigated in some way by diagenetic effects; conversely, alterations of the material structure may enhance swelling and creep effects during experimental tests. The effects of stress conditions and diagenetic processes experienced by the Argille del Santerno have been extremely heterogeneous due to its regional extension. Some samples from X-Ray Diffraction Analysis consistently show considerable percentages of quartz, calcite and dolomite as diagenesis markers. In fact, recrystallization and precipitation phenomena mainly involve quartz and carbonates grains, whereas the replacement process predominantly occurs via the transformation of calcite into dolomite (Favero et al., 2016).

Furthermore, the studies developed on an Adriatic offshore gas field by Cassiani and Zoccatelli (2000) and Hueckel et al. (2001) corroborate the hypothesis that lab compaction data could be overestimated compared to the *in-situ* behavior. Experimental evidence of this discrepancy is attributed to aging effects which could be missed by a standard lab test. Aging, or secondary compression for geological scale periods, was defined as a change in mechanical properties resulting from secondary compression under a constant external load (Lambe and Whuitman, 1969; Terzaghi et al., 1996). Sedimentary formations, subject to a constant *in-situ* stress level, generally experience a time-dependent deformation (secondary compression). When loaded above the *in-situ* effective stress over certain stress ranges, as in the case of gas or oil extraction, the material exhibits a much higher "apparent pre-compression stress", and also a much lower compressibility (Hueckel et al., 2001).

Cementation, diagenetic and aging effects, together with the scale effect, can explain the observed discrepancy between the lab data (at confining pressure coherent with depth) and the dynamic values at the well scale.

However, lab data are particularly significant when quantifying the effects of both confining pressures and acquisition techniques, in terms of induced strain magnitude. Static values are in the order of a few GPa and they suffer considerably from the effects of confining pressure; dynamic values can reach 5 GPa and are barely affected by the confinement. In agreement with the reference technical literature (Fjaer et al., 2008), the average ratio between the dynamic and static values at the specimen scale is in the order of 2–3, and it decreases from 2.8 to 1.9 as the confining stress increases from 10 to 20 MPa. In fact, the static and dynamic Young's moduli for clastic consolidated material converge to

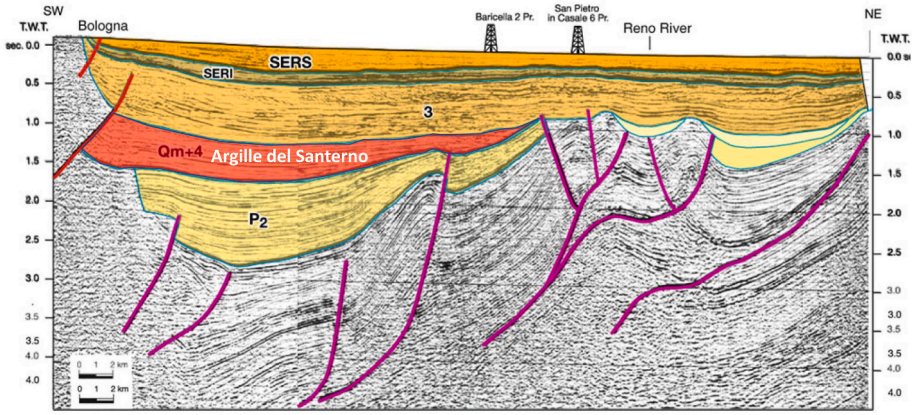

Fig. 17. Seismic line interpreted in the eastern Po Plain. Qm: Early Pleistocene (Argille del Santerno), 4: Yellow Sands, P2: Mid-Late Pliocene (fig. modified from Boccaletti et al., 2011).

their maximum values as the confining pressure increases. Furthermore, the comparison between E_D vs depth and the Baù et al. (2002) correlation proves consistent. Overall, lab data defined a rather homogeneous and well-predictable behavior, in line with the theoretical studies.

6. Conclusions

Our work was focused on the deformation behavior of the Argille del Santerno shales on the Po Plain (northern Italy), which are the caprock of numerous onshore and offshore gas reservoirs. Currently, depleted gas reservoirs are being considered for prospective underground storage of CO_2 and hydrogen. Thus, the need arises to characterize the shale deformation response to the stress variations induced by fluid injection and withdrawal.

The main results of our analysis of log and core data can be summarized as follows:

1. The Argille del Santerno Fm. exhibits a rather homogeneous and well-predictable deformation behavior;
2. In line with previous research and theoretical studies, the ratio between the dynamic Young's moduli (typically measured at the wells) and the static Young's moduli (typically measured in the lab) can reach an order of magnitude. Cementation, diagenetic and aging effects, together with scale effects, are responsible for this systematic discrepancy;
3. Deviations from the average values of static Young's moduli depend on the sampling procedures and laboratory testing conditions, which can alter the properties and the mechanical response of the *in-situ* undisturbed formation;
4. Young's modulus of the Argille del Santerno linearly increases with depth; an empirical relation was obtained to describe this correlation;
5. The analyses of the termination of the main thrust faults on the Po Plain show that the vertical continuity of the Argille del Santerno Fm. is not compromised by the presence of major faults.

Based on our correlation of Young's moduli with depth, the deformation characteristics of the Argille del Santerno can be predicted when lab or field data are lacking. The quantitative results obtained on the Young's modulus of the Argille del Santerno provide the input data needed for the geomechanical models which are then used to assess the potential impact and safety of underground operations. Thus, this work offers a valid contribution to making reservoir conversion into CO_2 e H_2 storage an achievable and socially acceptable option.

Credit authors statement

Christoforos Benetatos: Conceptualization, Formal analysis, Investigation, Methodology, Writing – original draft, Writing – review & editing, Supervision. Vera Rocca: Conceptualization, Formal analysis, Investigation, Methodology, Writing – original draft, Writing – review & editing, Supervision. Francesca Veraga: Writing-review & editing, Supervision. Luca Adinolfi: Review. Francesco Marzano: Review.

Declaration of competing interest

The authors declare that they have no known competing financial interests or personal relationships that could have appeared to influence the work reported in this paper.

Data availability

The authors do not have permission to share data.

Acknowledgments

The authors would like to thank all the anonymous reviewers for their constructive comments that improved the manuscript.

References

Ali, S.A., Clark, W.J., Moore, W.R., Dribus, J.R., 2010. Diagenesis and reservoir quality. Oilfield Rev. 22 (2), 14–27. ISSN 09231730.

Amadori, C., Garcia-Castellanos, D., Toscani, G., Sternai, P., Fantoni, R., Ghielmi, M., Di Giulio, A., 2018. Restored topography of the Po Plain-Northern Adriatic region during the Messinian base-level drop—implications for the physiography and compartmentalization of the palaeo-Mediterranean basin. Basin Res. 30, 1247–1263. https://doi.org/10.1111/bre.12302.

Amadori, C., Toscani, G., Di Giulio, A., Maesano, F.E., D'Ambrogio, C., Ghielmi, M., Fantoni, R., 2019. From cylindrical to non-cylindrical foreland basin: Pliocene–Pleistocene evolution of the Po Plain–Northern Adriatic basin (Italy). Basin Res. 31, 991–1015. https://doi.org/10.1111/bre.12369.

Antoncecchi, I., Ciccone, F., Rossi, G., Agate, G., Colucci, F., Moia, F., Manzo, M., Lanari, R., Bonano, M., De Luca, C., Calabrese, L., Perini, L., Severi, P., Pezzo, G., Macini, P., Benetatos, C., Rocca, V., Carminati, E., Billi, A., Petracchini, L., 2021. Soil deformation analysis through fluid-dynamic modelling and DInSAR measurements: a focus on groundwater withdrawal in the Ravenna area (Italy). Boll. Geof. Teor. Appl. 62, 301–316. https://doi.org/10.4430/bgta0350.

Baù, D., Ferronato, M., Gambolati, G., Teatini, P., 2002. Basin-scale compressibility of the northern Adriatic by the radioactive marker technique. Geotechnique 52 (8), 605–616. https://doi.org/10.1680/geot.2002.52.8.605.

Benetatos, C., Codegone, G., Marzano, F., Costanzo, P., Verga, F., 2019. Calculation of lithology-specific P-wave velocity relations from sonic well logs for the Po-Plain area and the northern Adriatic Sea. In: Proceedings of the Offshore Mediterranean Conference and Exhibition, Ravenna, Italy, 27–29 March 2019.

Benetatos, C., Giglio, G., 2021. Coping with uncertainties through an automated workflow for 3D reservoir modelling of carbonate reservoirs (Open Access). Geosci. Front. 12 (6) https://doi.org/10.1016/j.gsf.2019.11.008 art. no. 100913.

Benetatos, C., Bocchini, S., Carpignano, A., Chiodoni, A., Cocuzza, M., Deangeli, C., Eid, C., Gerboni, R., Lamberti, A., Marasso, S., Massimiani, A., Menin, B., Moscatello, A., Panini, F., Peter, C., Pirri, F., Quaglio, M., Rocca, V., Rovere, A., Salina Borello, E., Serazio, C., Uggenti, A.C., Vasile N- Verga, F., Viberti, D., 2021. How underground systems can contribute to meet the challenges of energy transition. GEAM 58, 65–80. https://doi.org/10.19199/2021.163-164.1121-9041.065, 2021.

Bertello, F., Fantoni, R., Franciosi, R., Gatti, V., Ghielmi, M., Pugliese, A., 2010. From thrust-and-fold belt to foreland: hydrocarbon occurrences in Italy. In: Vining, B.A., Pickering, S.C. (Eds.), Petroleum Geology: from Mature Basin to New Frontiers, Proceedings of the 7th Petroleum Geology Conference. Geological Society, London, pp. 112–113. https://doi.org/10.1144/0070113.

Bertotti, G., Picotti, V., Bernoulli, D., Castellarin, A., 1993. From rifting to drifting: tectonic evolution of the south-alpine upper crust from the triassic to the early cretaceous. Sediment. Geol. 86, 53–76. https://doi.org/10.1016/0037-0738(93)90133-P.

Boccaletti, M., Corti, G., Martelli, L., 2011. Recent and active tectonics of the external zone of the Northern Apennines (Italy). Int. J. Earth Sci. https://doi.org/10.1007/s00531-010-0545-y.

Bossart, P., Trick, T., Meier, P.M., Mayor, J.C., 2004. Structural and hydrogeological characterisation of the excavation-disturbed zone in the Opalinus clay (mont terri project, Switzerland). Appl. Clay Sci. 26 (Issues 1–4), 429–448. https://doi.org/10.1016/j.clay.2003.12.018. August 2004.

Bresciani, I., Perotti, C.R., 2014. An active deformation structure in the Po Plain (N Italy): the Romanengo anticline. Tectonics 33. https://doi.org/10.1002/2013TC003422.

Burland, J.B., 1990. On the compressibility and shear strength of natural clays. Geotechnique 40, 329–378. https://doi.org/10.1680/geot.1990.40.3.329.

Cardu, M., Giraudi, A., Rocca, V., Verga, F., 2012. Experimental laboratory tests focused on rock characterization for mechanical excavation. Int. J. Min. Reclamat. Environ. 26 (issue 3), 199–216. https://doi.org/10.1080/17480930.2012.712822. September 2012.

Carminati, E., Doglioni, C., 2012. Alps vs. Apennines: the paradigm of a tectonically asymmetric Earth. Earth Sci. Rev. 112, 67–96. https://doi.org/10.1016/j.earscirev.2012.02.004.

Carminati, E., Lustrino, M., Doglioni, C., 2012. Geodynamic evolution of the central and western Mediterranean: tectonics vs. igneous petrology constraints. Tectonophysics 579, 173–192. https://doi.org/10.1016/j.tecto.2012.01.026.

Casero, P., 2004. Structural setting of petroleum exploration plays in Italy. In: Crescenti, V., D'Offizi, S., Merlino, S., Sacchi, L. (Eds.), Geology of Italy. Special Volume of the Italian Geological Society for the IGC 32 Florence 2004. Societa` Geologica Italiana, pp. 189–199.

Castagna, J.P., Batzle, M.L., Kan, T.K., 1993. Rock physics—the link between rock properties and AVO response. In: Castagna, J.P., Backus, M.M. (Eds.), Offset-Dependent Reflectivity-Theory and Practice of AVO Analysis. Investigations in Geophysics Series,, vol. 8. Soc. Expl. Geophys., pp. 135–171

Cassiani, G., Zoccatelli, C., 2000. Towards a reconciliation between laboratory and in-situ measurements of soil and rock compressibility. In: Carbognin, L., et al. (Eds.), Land Subsidence (Proceedings of VI International Symposium on Land Subsidence), vol. II. La Garangola, Padua, Italy, pp. 3–15.

Castellarin, A., Eva, C., Ciglia, G., Vai, G.B., 1985. Analisi strutturale del Fronte Appenninico Padano. Giorn. Geol. 47 (1,2), 47–75.

Cazzini, F., Dal Zotto, O., Fantoni, R., Ghielmi, M., Ronchi, P., Scotti, P., 2015. Oil and gas in the Adriatic foreland, Italy. J. Petrol. Geol. 38, 255–279. https://doi.org/10.1111/jpg.12610.

Codegone, G., Rocca, V., Verga, F., Coti, 2016. Subsidence modeling validation through back analysis for an Italian gas storage field. Geotech. Geol. Eng. 34 (6), 1749–1763. https://doi.org/10.1007/s10706-016-9986-9.

Corkum, A.G., Martin, C.D., 2007. The mechanical behaviour of weak mudstone (Opalinus Clay) at low stresses. Int. J. Rock Mech. Min. Sci. 44 (2), 196–209. https://doi.org/10.1016/j.ijrmms.2006.06.004. February 2007.

Coti, C., Rocca, V., Sacchi, Q., 2018. Pseudo-elastic response of gas bearing clastic formations: an Italian case study. Energies 11, 2488. https://doi.org/10.3390/en11092488, 2018.

Darracott, B.W., Orr, C.M., 1976. Geophysics and rock engineering. In: Symp. On Exploration for Rock Engineering. Johannesburg, vol. 1, pp. 159–164 (Cape Town/Rotterdam: Balkema).

Dercourt, J., Zonenshain, L.P., Ricou, L.E., Kazmin, V.G., le Pichon, X., Knipper, A.L., Grandjacquet, C., Sbortshikov, I.M., Geyssant, J., Lepvrier, C., Pechersky, D.H., Biju-Duval, B., 1986. Geological evolution of the tethys belt from atlantic to the pamirs since the lias. In: Aubouin, J., LePichon, X., Monin, A.S. (Eds.), Evolution of the Tethys, vol. 123, pp. 241–315. https://doi.org/10.1016/0040-1951(86)90199-X issue 1-4.

Fantoni, R., Bersezio, R., Forcella, F., 2004. Alpine structure and deformation chronology at the southern Alps-Po plain border in Lombardy. Boll. Soc. Geol. Ital. 123 (3), 463–477. ISSN: 00378763.

Fantoni, R., Franciosi, R., 2009. Estensione mesozoica e compressione cenozoica nell'avampaese padano–adriatico. Abstract e Poster Natura e geodinamica della litosfera nell'alto Adriatico Venezia, PalazzoLoredan 5–6 Novembre 2009. Rend online Soc Geol It 9, 28–31 (in Italian).

Fantoni, R., Franciosi, R., 2010. Tectono-sedimentary setting of the Po Plain and adriatic foreland. Rend. Fis. Acc. Lincei 21 (1), 197–209. https://doi.org/10.1007/s12210-010-0102-4.

Favero, V., Ferrari, A., Laloui, L., 2016. On the hydro-mechanical behaviour of remoulded and natural Opalinus clay shale. Eng. Geol. 208, 128–135. https://doi.org/10.1016/j.enggeo.2016.04.030.

Ferronato, M., Gambolati, G., Teatini, P., Baù, D., 2002. Interpretation of radioactive market measurements to evaluate compaction in the norther Adriatic gas fields, 2003 SPE Reservoir Eval. Eng. 6 (6), 401–411. https://doi.org/10.2118/79470-PA. ISSN 10946470.

Fjaer, E., Holt, R.M., Horsrud, P., Raaen, A.M., Risnes, R., 2008. Petroleum Related Rock Mechanics, second ed. Elsevier, Amsterdam, p. 491. 9780444502605.

Gardner, G.H.F., Gardner, L.W., Gregory, A.R., 1974. Formation velocity and density—the diagnostic basics for stratigraphic traps. Geophysics 39 (6), 770–780. https://doi.org/10.1190/1.1440465.

Gautam, R., Wong, R.C., 2006. Transversely isotropic stiffness parameters and their measurement in Colorado shale. Can. Geotech. J. 43 (12), 1290–1305. https://doi.org/10.1139/T06-083.

Ghielmi, M., Minervini, M., Nini, C., Rogledi, S., Rossi, M., Vignolo, A., 2010. Sedimentary and tectonic evolution in the eastern Po-Plain and northern Adriatic Sea area from messinian to Middle Pleistocene (Italy). Rend. Fis. Acc. Lincei 21 (Suppl. 1), S131–S166. https://doi.org/10.1007/s12210-010-0101-5.

Ghielmi, M., Minervini, M., Nini, C., Rogledi, S., Rossi, M., 2013. Late Miocene–Middle Pleistocene sequences in the Po Plain–Northern Adriatic Sea (Italy): the stratigraphic record of modification phases affecting a complex foreland basin. Mar. Petrol. Geol. 42, 50–81. https://doi.org/10.1016/j.marpetgeo.2012.11.007.

Gibson, R.E., 1958. The progress of consolidation in a clay layer increasing in thickness with time. Geotechnique 8, 171–182. https://doi.org/10.1680/geot.1958.8.4.171.

Gong, F., Di, B., Zeng, L., Wei, J., Ding, P., 2020. Static and dynamic linear compressibility of dry artificial and natural shales under confining pressure. J. Pet. Sci. Eng. 192, 107242 https://doi.org/10.1016/j.petrol.2020.107242, 10.2475/ajs.s5-31.184.241.

Hong, Z.S., Zeng, L.-L., Cui, Y.J., Cai, Y.-Q., Lin, C., 2012. Compression behaviour of natural and remoulded clays. Geotechnique 62 (4), 291–301. https://doi.org/10.1680/geot.10.P.046.hal-00693382.

Hueckel, T., Cassiani, G., Tao, F., Pellegrino, A., Fioravante, V., 2001. Aging of oil/gas sediments their compressibility and subsidence. J. Geotech. Eng. 127 (11), 926–938. https://doi.org/10.1061/(ASCE)1090-0241(2001)127:11(926).

Islam, M.A., Skalle, P., 2013. An experimental investigation of shale mechanical properties through drained and undrained test mechanisms. Rock Mech. Rock Eng. 46, 1391–1413. https://doi.org/10.1007/s00603-013-0377-8.

Jardine, R.J., Symes, M.J., Burland, J.B., 1984. The measurement of soil stiffness in the triaxial apparatus. Geotechnique 34 (3), 323–340. https://doi.org/10.1680/geot.1984.34.3.323, 1984.

Jones, M.E., Addis, M.A., 1985. On changes in porosity and volume during burial of argillaceous sediments. Mar. Petrol. Geol. 2 (3), 247–253. https://doi.org/10.1016/0264-8172(85)90014-5.

Lambe, W.T., Whuitman, R.V., 1969. Soil Mechanics. John Wiley & Sons, ISBN 978-0-471-51192-2, p. 576.

Lancellotta, R., 2012. Geotecnica (4a Edizione), p. 544, 9788808059918 (in italian).

Livani, M., Petracchini, L., Benetatos, C., Marzano, F., Billi, A., Carminati, E., Doglioni, C., Petricca, P., Maffucci, R., Codegone, G., et al., 2023. Subsurface geological and geophysical data from the Po Plain and the northern Adriatic Sea (north Italy). Earth Syst. Sci. Data Discuss. 2023, 1–41. https://doi.org/10.5194/essd-2023-65.

Maesano, F.E., D'Ambrogi, C., Burrato, P., Toscani, G., 2015. Slip-rates of blind thrusts in slow deforming areas: examples from the Po Plain (Italy). Tectonophysics 643, 8–25. https://doi.org/10.1016/j.tecto.2014.12.007.

Maesano, F.E., D'Ambrogi, C., 2016. Coupling sedimentation and tectonic control: Pleistocene evolution of the central Po Basin. Italian J. Geosci. 135 (3), 394–407. https://doi.org/10.3301/IJG.2015.17.

Martínez-Martínez, J., Benavente, D., García-del-Cura, M.A., 2012. Comparison of the static and dynamic elastic modulus in carbonate rocks. Bull. Eng. Geol. Environ. 71 (2), 263–268. https://doi.org/10.1007/s10064-011-0399-y.

Marzano, F., Pregliasco, M., Rocca, V., 2020. Experimental characterization of the deformation behavior of a gas-bearing clastic formation: soft or hard rocks? A case study. Geomech. Geophys. Geo-Energy Geo-Resourc. 6 (1), 1–15. https://doi.org/10.1007/s40948-019-00130-3.

Picotti, V., Capozzi, R., Bertozzi, G., Mosca, F., Sitta, A., Tornaghi, M., 2007. The Miocene petroleum system of the northern Apennines in the central Po plain (Italy). In: Lacombe, O., Lavé, J., Roure, F., Vergés, J. (Eds.), Thrust Belts and Foreland Basins. From Fold Kinematics to Hydrocarbon Systems. Springer, Berlin, pp. 117–131. https://doi.org/10.1007/978-3-540-69426-7_6.

Picotti, V., Pazzaglia, F.J., 2008. A new active tectonic model for the construction of the Northern Apennines mountain front near Bologna (Italy). J. Geophys. Res. 113, B08412 https://doi.org/10.1029/2007JB005307.

Pieri, M., Groppi, G., 1981. Subsurface Geological Structure of the Po Plain, Italy, Progetto Finalizzato Geodinamica- Sottoprogetto 5- Modello Strutturale (Publ. 414). CNR, Roma.

Quattrone, P., Rogledi, S., Longoni, R., 1990. Gas fields in the tertiary sequences of the milano bergamo region. Bull. Swiss Assoc. of Petroleum Geol. And Eng. 56 (131), 53–64.

Rocca, V., Cannata, A., Gotto, A., 2019. A critical assessment of the reliability of predicting subsidence phenomena induced by hydrocarbon production. Geomech. Energy Environ. 20 https://doi.org/10.1016/j.gete.2019.100129.

Schmertmann, J.H., 1991. The mechanical aging of soils. J. Geotech. Eng. 117 (9), 1288–1330.

Skempton, A., 1969. The consolidation of clays by gravitational compaction. Q. J. Geol. Soc. 125, 373–411. https://doi.org/10.1144/gsjgs.125.1.0373.

Soler, J.M., 2001. The effect of coupled transport phenomena in the Opalinus Clay and implications for radionuclide transport. J. Contam. Hydrol. 53 (Issues 1–2), 63–84. https://doi.org/10.1016/S0169-7722(01)00140-1, 1 December 2001.

Teatini, P., Castelletto, N., Ferronato, M., Gambolati, G., Janna, C., Cairo, E., Marzorati, D., Colombo, D., Ferretti, A., Bagliani, A., Bottazzi, F., 2011. Geomechanical response to seasonal gas storage in depleted reservoirs: a case study in the Po River basin, Italy. J. Geophys. Res. 116, F02002 https://doi.org/10.1029/2010JF001793.

Terzaghi, K., Peck, R.B., Mesri, G., 1996. Soil Mechanics in Engineering Practice, third ed. John Wiley, New York. 0-471-08658-4.

Toscani, G., Bonini, L., Ahmad, M.I., Di Bucci, D.D., Di Giulio, A., Seno, S., Galuppo, C., 2014. Opposite verging chains sharing the same foreland: kinematics and interactions through analogue models (Central Po Plain, Italy). Tectonophysics 633 (1), 268–282. https://doi.org/10.1016/j.tecto.2014.07.019.

Turrini, C., Lacombe, O., Roure, F., 2014. Present-day 3D structural model of the Po Valley basin, Northern Italy. Mar. Petrol. Geol. 56, 266–289. https://doi.org/10.1016/j.marpetgeo.2014.02.006.

ViDEPI, 2023. Visibilità dei dati afferenti all'attività Di Esplorazione Petrolifera in Italia (Visibility of petroleum exploration data in Italy). Website. https://www.videpi.com/videpi/videpi.asp.